



Contents lists available at ScienceDirect

Chemical Engineering Research and Design

IChemE

journal homepage: [www.elsevier.com/locate/cherd](http://www.elsevier.com/locate/cherd)

## An overview on oxyfuel coal combustion—State of the art research and technology development

Terry Wall<sup>a,\*</sup>, Yinghui Liu<sup>a</sup>, Chris Spero<sup>b</sup>, Liza Elliott<sup>a</sup>, Sameer Khare<sup>a</sup>, Renu Rathnam<sup>a</sup>, Farida Zeenathal<sup>a</sup>, Behdad Moghtaderi<sup>a</sup>, Bart Buhre<sup>d</sup>, Changdong Sheng<sup>e</sup>, Raj Gupta<sup>f</sup>, Toshihiko Yamada<sup>c</sup>, Keiji Makino<sup>c</sup>, Jianglong Yu<sup>a,g</sup>

<sup>a</sup> CRC for Coal in Sustainable Development (CCSD), University of Newcastle, NSW 2308, Australia

<sup>b</sup> CCSD, CS Energy, Australia

<sup>c</sup> IHI, Japan

<sup>d</sup> Shell Development (Australia) Pty Ltd., Australia

<sup>e</sup> School of Energy and Environment, Southeast University, China

<sup>f</sup> Department of Chemical and Materials Engineering, University of Alberta, Canada

<sup>g</sup> Shenyang Institute of Aeronautical Engineering and University of Science and Technology, Liaoning, China

### A B S T R A C T

Oxyfuel combustion is seen as one of the major options for CO<sub>2</sub> capture for future clean coal technologies. The paper provides an overview on research activities and technology development through a fundamental research underpinning the Australia/Japan Oxyfuel Feasibility Project. Studies on oxyfuel combustion on a pilot-scale furnace and a laboratory scale drop tube furnace are presented and compared with computational fluid dynamics (CFD) predictions. The research has made several contributions to current knowledge, including; comprehensive assessment on oxyfuel combustion in a pilot-scale oxyfuel furnace, modifying the design criterion for an oxy retrofit by matching heat transfer, a new 4-grey gas model which accurately predicts emissivity of the gases in oxy-fired furnaces has been developed for furnace modelling, the first measurements of coal reactivity comparisons in air and oxyfuel at laboratory and pilot-scale; and predictions of observed delays in flame ignition in oxy-firing.

© 2009 The Institution of Chemical Engineers. Published by Elsevier B.V. All rights reserved.

**Keywords:** Oxyfuel coal combustion; CO<sub>2</sub> capture; Heat transfer; CFD prediction; Reactivity

### 1. Introduction

Energy production from fossil fuel combustion results in the emission of greenhouse gases, the dominant contributor being CO<sub>2</sub>. Public awareness and legislation have led to a policy of reduction of greenhouse gas emissions in most well-developed countries, with the regulations driven by international initiatives such as the Kyoto protocol and the Intergovernmental Panel on Climate Change (IPCC, 2007). Many talks have recently been held on post-Kyoto CO<sub>2</sub> trading schemes. Apart from increasing usage of renewable energy sources and nuclear power, the rapidly increasing global energy demand is expected to be met by conventional fossil fuels. Reduction of greenhouse gas emission from fossil fuel-

fired power generation can be achieved by efficiency improvement, switching to lower carbon fuels and CO<sub>2</sub> capture and storage (CCS) (Wall, 2005). A recent report released by MIT indicates CO<sub>2</sub> capture and storage is necessary for the future use of coal when carbon costs are established (Katzner, 2007).

There are several options for capture and storage of CO<sub>2</sub> from coal combustion and gasification, including:

- *Post-combustion capture:* CO<sub>2</sub> capture from conventional pulverised coal-firing plant with scrubbing of the flue gas by chemical solvents, solid minerals etc.
- *Pre-combustion capture:* Integrated gasification combined cycle (IGCC) with a shift reactor to convert CO to CO<sub>2</sub>, followed by CO<sub>2</sub> capture.

\* Corresponding author. Tel.: +61 2 49 216179; fax: +61 2 49 216920.  
E-mail address: [Terry.Wall@newcastle.edu.au](mailto:Terry.Wall@newcastle.edu.au) (T. Wall).

Received 21 August 2008; Received in revised form 25 November 2008; Accepted 16 February 2009

0263-8762/\$ – see front matter © 2009 The Institution of Chemical Engineers. Published by Elsevier B.V. All rights reserved.  
doi:10.1016/j.cherd.2009.02.005

### Nomenclature

AFT	adiabatic flame temperature
CFD	computational fluid dynamic
DTF	drop tube furnace
FEGT	furnace exit gas temperature
IFRF	International Flame Research Foundation
TGA	thermogravimetric analysis
Type-0 and type 2-flames	identified by the IFRF, these are for forward flowing jet flames and flames with international recirculation respectively
WSGGM	weighted sum of gray gases model
WSM	well-stirred model, a simple mass and heat balance for a furnace

- *Oxyfuel combustion*: Combustion in oxygen rather than air, with recycled flue gas.
- *Chemical looping combustion*: Oxygen carried by solid oxygen carriers reacts with fuel to produce a high concentration CO<sub>2</sub> stream in the flue gas, oxygen carriers are then regenerated to uptake oxygen from air in a second reactor.

This review is focused on the science underpinning oxyfuel combustion technology.

Conventional pf coal-fired boilers, i.e., currently being used in power industry, use air for combustion in which the nitrogen from the air (approximately 79% by volume) dilutes the CO<sub>2</sub> concentration in the flue gas. During oxyfuel combustion, a combination of oxygen (typically of greater than 95% purity) and recycled flue gas is used for combustion of the fuel. A gas consisting mainly of CO<sub>2</sub> and water is generated with a concentration of CO<sub>2</sub> ready for sequestration. The recycled flue gas is used to control flame temperature and make up the volume of the missing N<sub>2</sub> to ensure there is enough gas to carry the heat through the boiler. A general flow sheet is shown in Fig. 1. CO<sub>2</sub> capture and storage by the current technically viable options post-combustion capture, pre-combustion capture and oxyfuel combustion will impose a 7–10% efficiency penalty on the power generation process. The major contributors to this efficiency penalty are oxygen production and CO<sub>2</sub> compression.

The concept of oxyfuel combustion was proposed in 1982 by Abraham in the context of providing a CO<sub>2</sub>-rich flue gas for enhanced oil recovery (Abraham et al., 1982). Due to these potential benefits, Argonne National Laboratory (ANL) carried out some research activities including a techno-economic study and pilot-scale studies (Weller et al., 1985; Berry and Wolsky, 1986; Wang et al., 1988; Abele et al., 1987). During the early 1990s, because of interest in capturing CO<sub>2</sub> from coal combustion, IFRF performed the first oxy-coal combustion with RFG (recirculated flue gas) in a pilot-scale study in Europe, NEDO initiated a study on oxy-coal combustion with RFG, to allow consideration of retrofitting Japanese boilers with the technology. Combustion trials were completed by IHI (Nozaki et al., 1997; Kiga et al., 1997; Kimura et al., 1995; Nakayama et al., 1992). During the late 1990s, CANMET and a research consortium led by Babcock and Wilcox and Air Liquide did further pilot-scale studies. Based on these developments, oxy-fuel technology has now evolved from pilot-scale to several planned demonstration scale projects.

The literature contains many reviews of the development of the technology (Wall, 2005; Santos et al., 2006; Croiset et al.,

2005; White et al., 2003; Kiga, 2001; Allam et al., 2005; Buhre et al., 2005). Thus this review is scoped on original R&D research activities on a fundamental level carried out at the University of Newcastle under the framework of a joint Australia–Japan Callide A Oxyfuel feasibility study, updating the state-of-the-art oxyfuel technology reviewed in 2005 (Buhre et al., 2005) and 2007 (T.F. Wall, 2007) respectively. The most important consideration of the paper is the understanding of the differences between oxyfuel combustion and conventional combustion, including heat transfer, coal reactivity and emissions. The current paper presents research in these areas, which has most relevance to a boiler retrofit. Compared with the other two reviews published from this group, the current review emphasis is scientific understanding of the oxyfuel technology, rather than the previous technical point of view. Research conducted within the scope of the current paper has primarily been presented at international conferences and published as journal papers (Wall, 2005; T. Wall, 2007; T.F. Wall, 2007; Rathnam et al., 2006, 2007; S.P. Khare et al., 2007; Khare et al., 2008; Yamada et al., 2006; Lundstöm et al., 2006; Gupta et al., 2006; Spero, 2007).

## 2. Differences between air and oxyfuel combustion conditions

From pilot-scale and laboratory scale experimental studies, oxyfuel combustion has been found to differ from air combustion in several ways, including reduced flame temperature, delayed flame ignition, reduced NO<sub>x</sub> and SO<sub>x</sub> emissions.

Many of these effects can be explained by differences in gas properties between CO<sub>2</sub> and N<sub>2</sub>, the main diluting gases in oxyfuel and air respectively. CO<sub>2</sub> has different properties from N<sub>2</sub> which influence both heat transfer and combustion reaction kinetics:

- *Density*: The molecular weight of CO<sub>2</sub> is 44, compared to 28 for N<sub>2</sub>, thus the density of the flue gas is higher in oxyfuel combustion.
- *Heat capacity*: The heat capacity of CO<sub>2</sub> is higher than N<sub>2</sub>.
- *Diffusivity*: The oxygen diffusion rate in CO<sub>2</sub> is 0.8 times that in N<sub>2</sub>.
- *Radiative properties of the furnace gases*: Oxyfuel combustion has higher CO<sub>2</sub> and H<sub>2</sub>O levels, both having high emitting power.

The following list identifies differences for oxy-firing compared to air-firing:

- To attain a similar adiabatic flame temperature (AFT) the O<sub>2</sub> proportion of the gases passing through the burners is higher, typically 30%, than that for air (of 21%), necessitating that about 60% of the flue gas is recycled.
- The high proportions of CO<sub>2</sub> and H<sub>2</sub>O in the furnace gases result in higher gas emissivities, so that similar radiative heat transfer for a boiler retrofitted to oxyfuel will be attained when the O<sub>2</sub> proportion of the gases passing through the burner is less than the 30% required for the same AFT.
- The volume of gases flowing through the furnace is reduced by which the extent is dependent on the flue gas recycle ratio, and the volume of flue gas emitted from power plant is reduced by about 80%.
- Typically, when air-firing coal, 20% excess air is used. Oxy-fuel requires a percent excess O<sub>2</sub> (defined as the O<sub>2</sub> supplied in excess of that required for stoichiometric combustion of

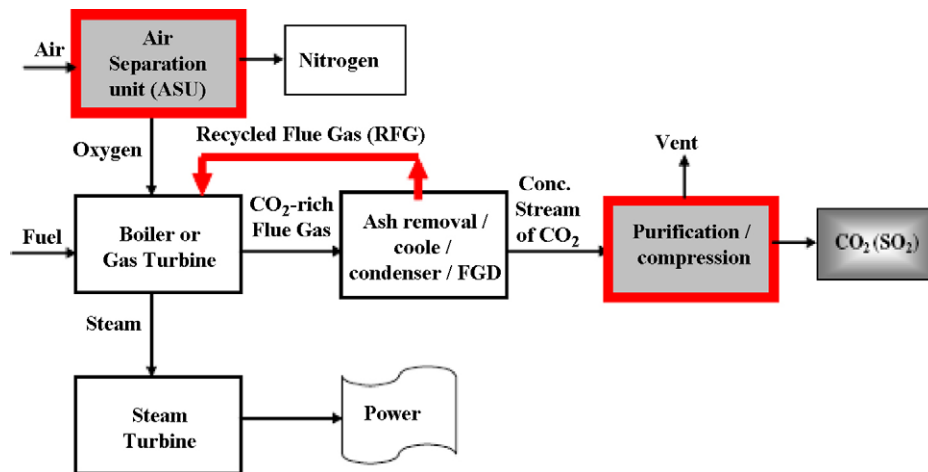


Fig. 1 – Flowsheet of oxyfuel technology for power generation with CO<sub>2</sub> capture and storage, showing the additional unit operations in bold.

the coal supply) to achieve a similar O<sub>2</sub> fraction in the flue gas as air-firing, in the range of 3–5%.

- Due to the recycling of flue gases to the furnace, species (including corrosive sulphur gases) have higher concentrations than in air-firing, if these species are not removed prior to recycle.
- As oxyfuel combustion combined with sequestration must provide power to several significant unit operations, such as flue gas compression, that are not required in a conventional plant without sequestration, oxyfuel combustion/sequestration is less efficient per unit of energy produced.

### 3. Pilot-scale furnace experiments

#### 3.1. Furnace and experimental details

A simulation of the oxyfuel process requires a recycled gas stream of multiple species and multiple concentration levels, which is difficult to achieve at laboratory scale. Thus the 150 kg/h IHI combustion test facilities in Aioi, Japan was therefore used to test three Australian pulverised coals under both

oxyfuel and air combustion conditions. In such a furnace flue gas recycling is well simulated. The purpose of these tests was to obtain design data on flame stability, combustion characteristics, gaseous emissions, fly ash characteristics, and plant operation including turndown, and to provide data for fundamental interpretation and mathematical modelling. Here, differences and trends are identified and the data will be interpreted in the latter sections in a greater detail.

A direct comparison of oxyfuel and air combustion was made, with coals fired at the same throughput, same flue O<sub>2</sub> concentration, and the same average O<sub>2</sub> through the burners. The average O<sub>2</sub> through the burners was 27% (wet), in an attempt to establish the same heat transfer. A lower adiabatic flame temperature (AFT) for the oxyfuel conditions result.

Three coals were tested in the pilot-scale furnace in Aioi, with properties given in Table 1. The laboratory experiments were undertaken on size cuts of the same coals, with properties given in Table 2.

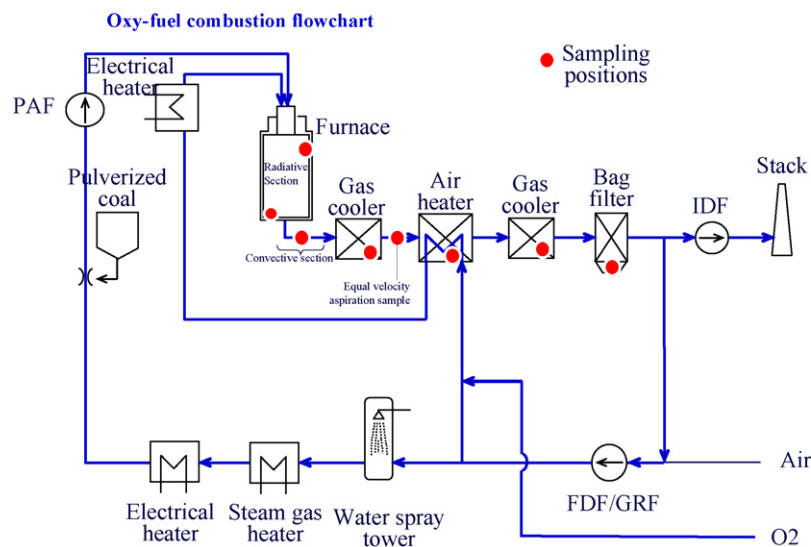
The Aioi test facility is a vertical, down fired furnace with a swirled single-burner, as illustrated in Fig. 2. The flue gas recycle rate during oxy-firing is set to obtain a nominal O<sub>2</sub> in the flue of 3% and wind-box O<sub>2</sub> of 35%. The selection of 3% oxygen in the flue gas is based on the level of excess oxy-

Table 1 – Analysis of coals used in pilot-scale tests.

		Coal A HHV = 23.7 dry MJ/kg	Coal B HHV = 27.9 dry MJ/kg	Coal C HHV = 30.0 dry MJ/kg
Proximate analysis				
I.M.	[a.d.%]	8.8	4.1	14.0
Ash	[dry%]	19.3	18.2	6.9
V.M.	[dry%]	25.7	40.9	34.1
F.C.	[dry%]	55.0	40.9	59.0
Ultimate analysis				
C	[dry%]	63.5	65.6	74.4
H	[dry%]	2.8	5.3	4.2
N	[dry%]	0.73	0.72	1.91
O	[dry%]	13.5	9.7	11.8
S	[dry%]	0.24	0.57	0.88
Ash analysis				
SiO <sub>2</sub>	[wt%]	47.6	65.7	45.7
Al <sub>2</sub> O <sub>3</sub>	[wt%]	28.6	28.5	22.0
Fe <sub>2</sub> O <sub>3</sub>	[wt%]	16.0	1.05	19.4
CaO	[wt%]	1.64	0.37	3.79
MgO	[wt%]	1.12	0.34	2.09
TiO <sub>2</sub>	[wt%]	2.22	2.19	0.75

**Table 2 – Proximate and ultimate analysis of the size cuts of the Coals A, B and C used in laboratory experiments.**

	Coal A (+63–90 $\mu\text{m}$ )	Coal B (+63–90 $\mu\text{m}$ )	Coal C (+63–90 $\mu\text{m}$ )
Proximate analysis wt% (air dried basis)			
Air-dried moisture	8.0	1.7	5.9
Ash (a.d.)	19.9	19.6	5.0
Volatile matter (a.d.)	25.6	40.5	33.8
Fixed carbon (a.d.)	46.5	38.2	55.3
Ultimate analysis wt% (dry ash free basis)			
Carbon	79.1	81.6	78.4
Hydrogen	4.51	6.84	5.13
Nitrogen	1.16	1.26	2.14
Sulphur	0.24	0.64	0.52
Oxygen	15.0	9.7	13.8

**Fig. 2 – Schematic of the IHI combustion test facility, indicating the unit-operations and sampling positions of deposits in the furnace, and gas and solids in the post-furnace operations.**

gen commonly experienced in air combustion boilers in steam power plants. By fixing the oxygen concentration in the flue gas and then tuning the recycle ratio of the flue gas, the oxygen concentration at the burner inlet can be adjusted. The resulting stoichiometric ratio in oxyfuel is less than that used in air combustion. This established the average  $\text{O}_2$  through the burner at 27%, a condition predicted by theory where the furnace heat transfer is matched with the heat transfer during air-firing. Mill conditions were set to achieve a nominal pulverised coal fineness of 75% mass  $<75 \mu\text{m}$ . Other conditions are given in Table 3, which indicates  $\text{O}_2$  levels and the three thermal inputs used to study turndown.

### 3.2. Measurements

Flame temperatures were measured by a radiation thermometer corrected to the estimated gas emissivity. In the dimension range of the test furnace, gas emissivity increases from 0.45 in air combustion to 0.55 in oxyfuel combustion. Details of the temperature measurement correction for gas emissivity are described elsewhere (Khare et al., 2008). Fig. 3 shows a comparison between air combustion and oxygen combustion temperature profiles for Coal A after the oxyfuel flame temperature was corrected. For all coals, the maximum flame temperature in air combustion was typically 100–150 °C higher

**Table 3 – Pilot-scale measurements, overall heat transfer prediction and measured by cooling water temperature rise.**

	Coal					
	A		B		C	
	Air	Oxy	Air	Oxy	Air	Oxy
Well-stirred model						
Estimated furnace heat transfer (kW)	348	354	368	373	342	347
Estimated heat flux ( $\text{kW}/\text{m}^2$ )	12.6	12.8	13.3	13.5	12.3	12.5
% difference, change from air to oxy	+1.6%	+1.5%	+1.6%			
Water-side heat balance						
	Using water flow $\sim 25 \text{ T/h}$					
Water inlet temperature ( $^{\circ}\text{C}$ )	37.8	38.1	32.8	34.2	-NA	-NA
Water exit temperature ( $^{\circ}\text{C}$ )	47.5	49.1	40.9	44.0	-NA	-NA
Estimated furnace heat absorption (kW)	354	392	336	356	-NA	-NA

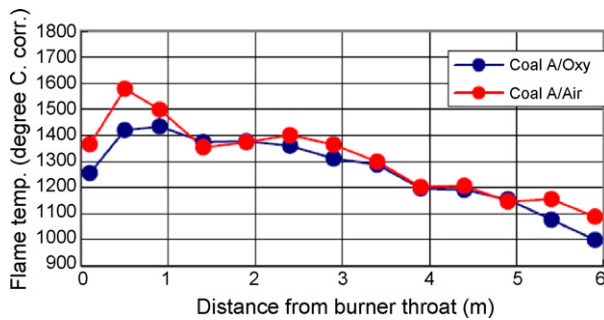


Fig. 3 – Gas temperature profiles measured by radiation pyrometry for Coal A.

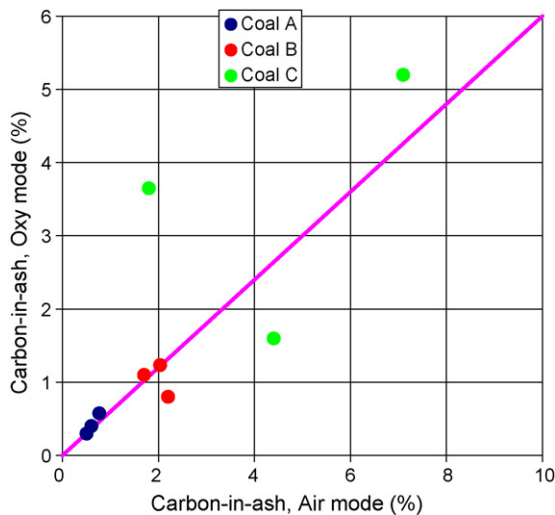


Fig. 4 – Carbon-in-ash comparisons for oxy mode and air mode. The unbroken line shows the trend of lower carbon in ash during oxyfuel combustion and the broken line represents parity.

than the oxyfuel flame temperature, and the furnace exit gas temperature (FEGT) was also higher in about 50 °C.

CO<sub>2</sub> concentration at the heat exchanger inlet in oxyfuel combustion was 70–80 dry%. This low value is because of a substantial air ingress from the devices such as the furnace, gas cooler and heat exchanger due to operations at an in-furnace pressure of about –0.1 kPa.

Fig. 4 shows the analysis results of carbon-in-ash in fly ash (determined by loss on ignition) collected using iso-kinetic sampling at the heat exchanger inlet. Oxyfuel combustion produced a relatively lower carbon-in-ash for Coal A and Coal B though the value of carbon-in-ash fluctuates in Coal C, apparently due to operational fluctuations. Overall, the carbon-in-ash for oxyfuel combustion was approximately 40% lower than for air combustion.

Flame conditions during the combustion test were adjusted via a single air register around the burner with photographs and a visual record used to identify differences in ignition location. The oxy-flames ignited at a greater distance from the burner. At low load operation, the oxy-flames were seen to ignite at a substantially greater distance from the burner.

#### 4. Heat transfer

Furnace heat transfer depends on flame temperature, heat transfer properties of gases and particulates, water cooling wall temperature and properties, and the aerodynamic fluid field established, including the flame types.

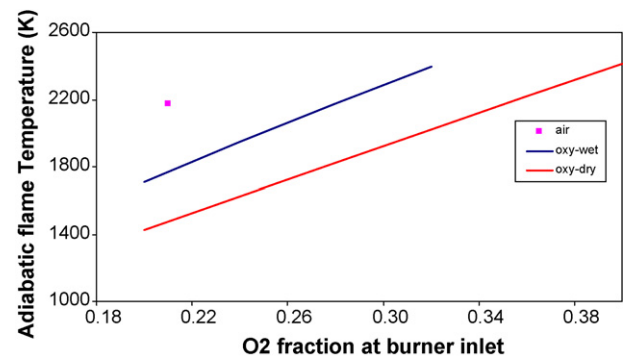


Fig. 5 – The O<sub>2</sub> partial pressure (fraction) required at burner inlet (to achieve similar adiabatic flame temperature as the air-fired case) for oxy-wet and oxy-dry (with 3.3% (v/v) O<sub>2</sub> in the flue gas).

The adiabatic flame temperature (AFT) of coal combustion in high oxygen concentrations is extremely high due to the lack of N<sub>2</sub> dilution. But the AFT of coal combustion in 21% oxygen with CO<sub>2</sub> dilution is lower than air combustion because of the higher heat capacity of CO<sub>2</sub>. By adjusting the ratio of recycled flue gas and thereby the oxygen concentration at the burner inlet, an adiabatic flame temperature similar to air combustion can be achieved; approximately 30% O<sub>2</sub> at the burner inlet. For a retrofit, to minimize changes in the current combustion system requires selection of an oxygen concentration at the burner inlet by selecting a ratio of recycled flue gas, which will vary depending on if the flue gas is dried, to achieve similar heat transfer as air combustion. Fig. 5 compares the adiabatic flame temperature for air and oxy-retrofit combustion where the AFT for air combustion is estimated for 20% excess air and O<sub>2</sub> levels in the flue gas at 3.3% (v/v). The feed condition for the combustion air includes primary flow (at 360 K) and secondary flow (560 K). The two oxy-retrofit combustion cases included in the figure are: oxy-wet recycle where the recycled flue gas includes water vapour, and oxy-dry recycle where water vapour is removed from the recycled flue gas. Under similar boundary conditions as air combustion, such as the same coal feed rate and combustion gas temperatures, the computation results show that the % excess O<sub>2</sub> required to maintain O<sub>2</sub> levels in the flue gas similar to air combustion is in the range of 3–5% for both oxy-dry and oxy-wet combustion. Similar levels of adiabatic flame temperatures (compared to air combustion) can then be established by changing the O<sub>2</sub> levels at the burner inlet (after recycle) through adjustment of the amount of recycled flue gas for oxy-wet and oxy-dry cases. From Fig. 5, to achieve the same AFT as the air combustion included in the figure, the O<sub>2</sub> fraction at the burner inlet for oxy-wet and oxy-dry combustion is approximately 28% or 35% for wet and dry recycle respectively. Partial drying of the recycled gas will give AFTs between these values.

For a retrofit furnace, the heat transfer produced during oxyfuel combustion must match the heat transfer during air combustion. This constraint is due to the amount of steam required to drive the steam turbine. Radiation is the principal mode of heat transfer in coal-fired furnaces. The main combustion products that actively participate in radiative heat transfer are CO<sub>2</sub>, H<sub>2</sub>O and particulate matter such as char, soot and fly ash particles. The furnace gases in oxyfuel combustion have much higher levels of CO<sub>2</sub>, H<sub>2</sub>O and a different CO<sub>2</sub>/H<sub>2</sub>O ratio to air combustion, and, due to lower gas volumes, higher particulate matter concentrations than air combustion. Thus

gas emissivities are higher for oxyfuel combustion, making AFT matching an invalid design criterion, because lower AFTs are required for an oxy retrofit.

Furnace design is traditionally made using design plots based on previous experience. For oxyfuel combustion, this is not the case and therefore computational fluid dynamic (CFD) is used as a design tool.

Although radiative properties of CO<sub>2</sub>, H<sub>2</sub>O and particulate matter have been established for air combustion, there is uncertainty regarding their validity for oxyfuel combustion systems. Currently CFD models (such as Fluent) employ a 3-gray-gas based weighted sum of gray gas model (WSGGM) to evaluate gas emissivity, which is not adequate for the high CO<sub>2</sub> and H<sub>2</sub>O concentrations in oxyfuel combustion. Thus a modified WSGGM model which introduces an extra gray gas component in the model has been developed for oxyfuel combustion to predict the local absorption coefficient and model coefficients suitable for the oxyfuel gas environment. This part of the work has been reported in (Gupta et al., 2006).

The total emissivity for combustion gases is estimated from Hottel's Charts (Hottel and Sarofim, 1967) in which the total emissivity is presented as a function of temperature, pressure and concentration of gases, and geometric path length of the system by combustion engineers. These charts were prepared for a limited range. However, some scaling rules for the total absorptivity and emissivity of combustion gases can be used to extend the range of applicability of Hottel's charts. However, the original charts were in error at conditions based on extrapolation of experimental data. Therefore, new charts were prepared by Leckner (1972) and Ludwig et al. (1973) based on the integration of measured spectral radiation data. Also, the scaling rules given by Edwards and Matavosian (1984) may be used to predict the gas emissivity at different pressures as well as gas absorptivity for different wall temperatures and at gas pressures different than one atmosphere. These charts were prepared using experimental data and were extended in range using wide band models or narrow band models (Hottel and Sarofim, 1967).

The total emissivity for the WSGGM is given by the following equation (Smith et al., 1982):

$$\varepsilon = \sum_{i=0}^I a_{\varepsilon,i}(T)[1 - e^{-k_i PS}] \quad (1)$$

where:  $a_{\varepsilon,i}$ , emissivity weighting factor for  $i$ th gray gas as based on gas temperature  $T$ ;  $[1 - e^{-k_i PS}]$ ,  $i$ th gray gas emissivity with absorption coefficient ( $k_i$ );  $PS$ , partial pressure-path length product (atm-m);  $P$ , sum of the partial pressures of the absorbing gases (atm);  $S$ , path length (m);  $k_i$ , absorption coefficient of  $i$ th gray gas (atm-m)<sup>-1</sup>;  $I$ , the number of gray gases.

The absorption coefficient for  $i=0$  (clear gas) is assigned a value of zero to account for gaps (windows) in the spectrum between spectral regions of high absorption. A convenient representation of the temperature dependency of the weighting factors is a polynomial of order  $J - 1$  given as follows:

$$a_{\varepsilon,i} = \sum_{j=1}^J b_{\varepsilon,i,j} T^{j-1} \quad (2)$$

where  $b_{\varepsilon,i,j}$ , emissivity gas temperature polynomial coefficients;  $J$ , the number of temperature polynomial coefficients

Fig. 6 indicates that Smith's constants, presented as the gray gas model (GGM), are not adequate even for an air-fired system for geometric path lengths larger than 10 m. That is, the wide band model (WBM) deviates from the GGM at higher

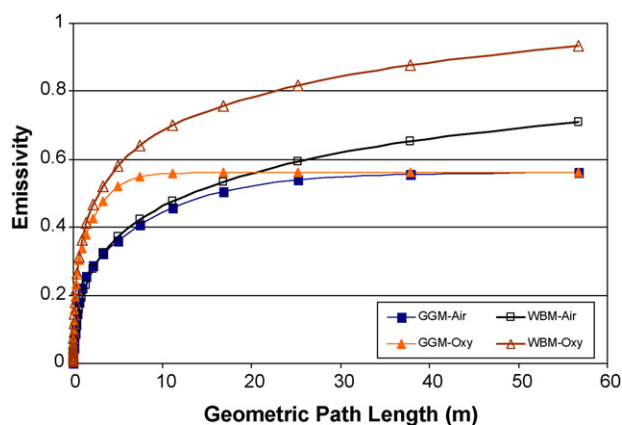


Fig. 6 – Comparison of emissivities at 1500 K for air-fired and oxy-fired systems estimated from WSGGM (with three grey gases and Smith's constants for  $P_w/P_c = 1$ ) and WBM for  $P_w/P_c = 0.5$ .

path lengths. These differences are much larger for oxy-firing systems even at a path length of 2–4 m. This demonstrates the need for an extra gray gas for larger combustion systems, in particular for oxy-firing systems. The new coefficient developed for 4-grey gas model is recently published in Khare's doctoral thesis (2008) (Khare, 2008).

Solid combustion products such as fine ash particles contribute to radiative heat transfer. Factors including the ash concentration, particle size distribution of cloud and the complex refractive index and absorption index play a role (Gupta and Wall, 1985). A simplified engineering approach is used to estimate the emissivity of a particulate cloud, as mentioned by Gupta and Wall (1985). The total emissivity due to joint emission from gas and particulate ash is shown in Table 4. Results in Table 4 clearly show changes in total emissivity with furnace size. As the scale is increased, there is a significant increase in gas emissivity. A stronger decrease of adiabatic flame temperature is required to compensate for the gain in emissivity. The increase in unit size also gives rise in particle radiation, and as the furnace volume emissivity gradually approaches one, the performance is no longer sensitive to changes of flue gas composition.

Table 4 – Estimates of ash, gas and combined emissivities in three furnaces of different scales, for Coal A, with no drying of recycle stream, or full drying in three furnaces of different scale.

	Furnace		
	F-A	F-B	F-C
Unit rating	0.2 MWt	30 MWe	420 MWe
Ash emissivity, $\varepsilon_{ash}$ (–)			
Air	0.02	0.22	0.47
Oxy-dry	0.04	0.34	0.66
Oxy-wet	0.03	0.28	0.58
Gas emissivity, $\varepsilon_g$ (–)			
Air	0.13	0.35	0.47
Oxy-dry	0.22	0.47	0.60
Oxy-wet	0.29	0.58	0.71
Combined emissivity, $\varepsilon_{Comb}$ (–)			
Air	0.16	0.49	0.72
Oxy-dry	0.25	0.65	0.86
Oxy-wet	0.31	0.70	0.88

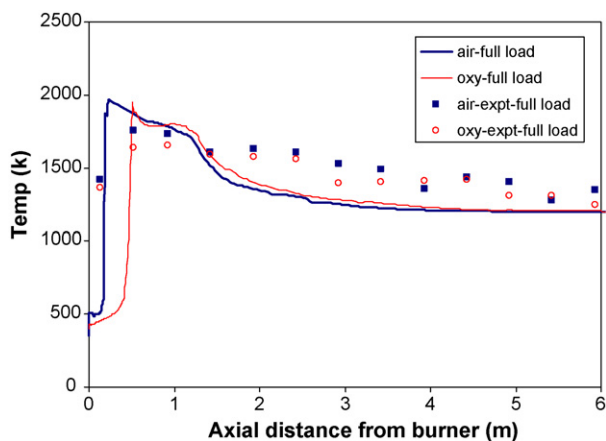


**Fig. 7 – Predicted maximum radial temperature variation with axial location and measured pyrometer temperature for full load operation.**

To study detailed burner geometry and the effect of coupled flow patterns during coal combustion on heat transfer in the furnace, a Fluent based CFD simulation has been developed and used to compare air and oxyfuel combustion situations, where the air burner is also used for the oxy-firing (Khare et al., 2008; S. Khare et al., 2007).

The predictions from the Fluent CFD model for the pilot-scale furnace include oxygen distribution inside the furnace, gas temperatures, particle residence times, gas velocities, gas species profiles, and furnace heat transfer. Predictions are given in Figs. 7–9.

Predictions indicate the flames in the pilot-scale furnace were of Type-0, that is, velocities in the flame jet are forward, and there is no internal recirculation. For all flames ignition was predicted to occur off-axis, at a radial distance of about 0.05 m from the burner centre line. The predicted axial location for ignition and peak (or maximum) temperature is different for air combustion and oxyfuel combustion, with oxy-conditions having a delayed ignition. Figs. 7 and 8 show model predictions for the gas temperature during full and partial load operation comparing air and oxyfuel combustion. In both cases, the partial load operation shows delayed ignition compared to full load operation, as observed during the experiments. The model indicates this is due to the higher ratio of momentum flux because of the larger relative mass flow rate of primary air/RFG, the effect of secondary gas swirl is then

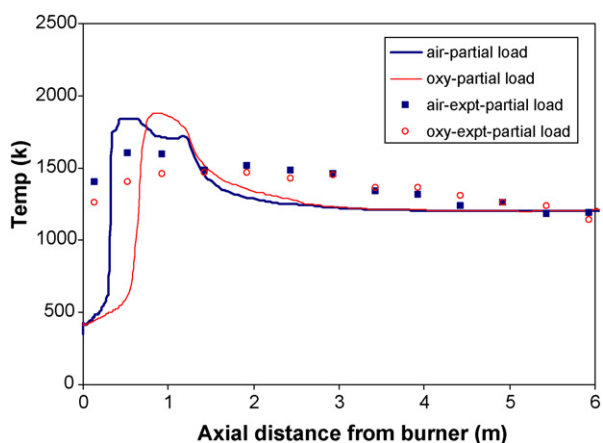


**Fig. 8 – Predicted maximum radial temperature variation with axial location and measured pyrometer temperature for partial load operation.**

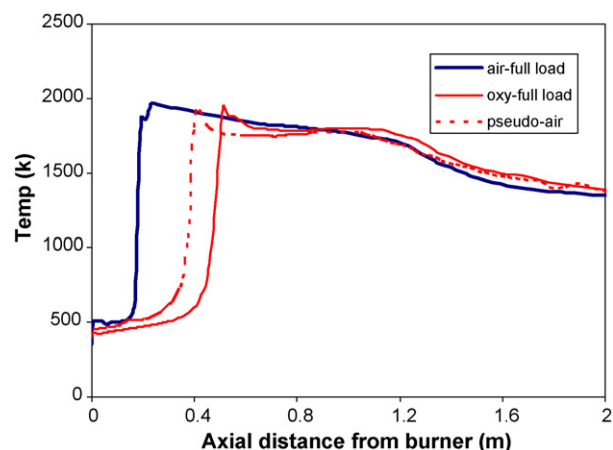


**Fig. 9 – Predicted axial temperature profiles for air and oxy-firing with pseudo-air, where oxy-firing has the same primary and secondary momentum as the air-firing.**

less significant. A theoretical analysis was also undertaken for oxyfuel in which the ratio of primary to secondary momentum flux is set at the level as air combustion (here, called pseudo-air). This is to understand the influence of gas composition alone on ignition location. However, other changes result. In the pseudo-air case, the secondary gas flow is increased by about 25% to match the momentum flux ratio as in air combustion, with no change in primary flue gas rate. The higher recirculated flue gas mass flow results in a lower average  $O_2$  concentration for the burner flows, reduced from 27 to 23% (v/v) at the burner inlet, also results in a lower adiabatic flame temperature and therefore a lower gas temperature. The predicted peak gas temperature for the pseudo-air combustion is thereby reduced by approximately  $50^\circ C$  when compared with the oxyfuel combustion, as given in Fig. 9. As shown in Fig. 9, the predicted ignition is located closer to the burner but does not match the air combustion ignition position. This is due to the different gas properties. Thus, the ignition delay in oxy-fuel combustion can be explained by the combined effect of the properties of combustion gases and aerodynamic impacts.

In the pilot-scale tests, all flames are Type-0. However; practical air combustion flames are commonly Type-2 swirled flames involving both internal as well as an external recirculation. For a retrofit application, when the burner flows are reduced during oxyfuel combustion, the flow velocities and therefore, the momentum flux ratio (the ratio of secondary to primary flow momentum) are lower, and the possibility exists that practical Type-2 air flames could become Type-0 oxyfuel flames. Changes to the burner dimensions and/or to the extent of swirling flow may then therefore be required to maintain a similar flame. Otherwise, a new burner specifically designed for oxyfuel combustion is required.

This furnace heat absorption is the primary design consideration (Payne et al., 1989). The well-mixed furnace model has therefore been used to compare impact of dry/wet recycle on requirement of  $O_2$  concentration at burner inlet (Khare et al., 2005).

To study the flames formation in a utility scale furnace, the 30 MWe furnace identified as F-B in Table 4, was modelled using a three-dimensional FLUENT model. All the flames predicted were Type-2, but the oxyfuel flame was more elongated, extending to the rear wall, as shown in Fig. 10. The overall furnace heat transfer between air combustion and oxyfuel combustion in a retrofitted furnace can be matched, however,

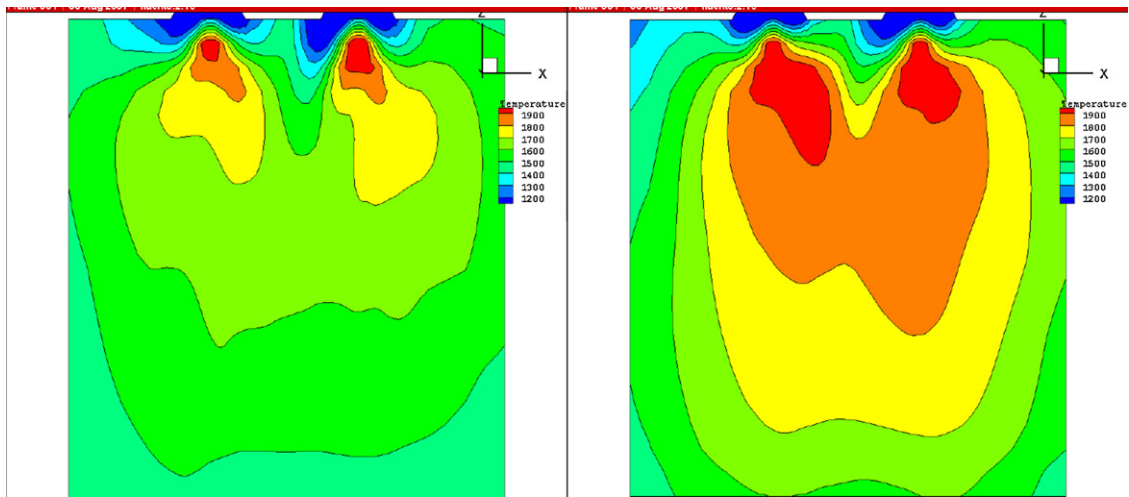


Fig. 10 – Predicted horizontal burner plane for air case (left) compared to the Oxy case (right) for a 3-MWe furnace.

the wall heat transfer distribution differs for air and oxyfuel combustion as shown in Fig. 11. The furnace wall heat transfer distribution shows higher heat transfer on the burner wall compared to the rear wall for the air combustion. However,

for oxyfuel combustion, the rear wall heat transfer was higher due the effect of the longer flame. When the momentum ratios of primary to secondary flows in oxyfuel combustion were matched to those in air combustion (pseudo-air combus-

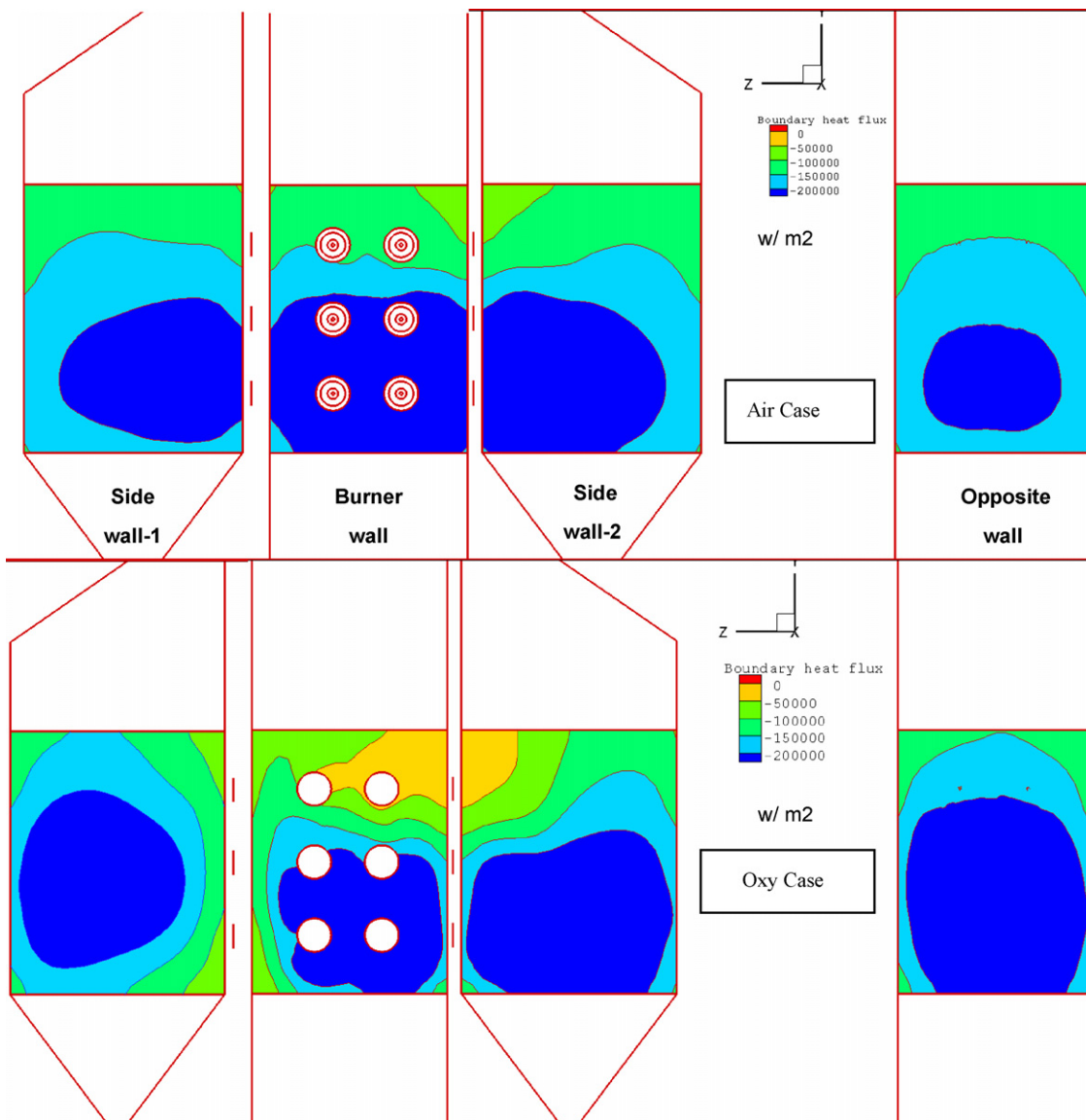
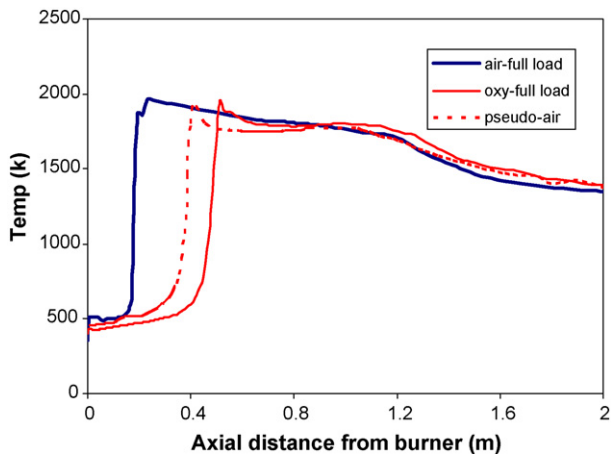


Fig. 11 – Folded furnace wall heat flux contours for air and oxy case, showing higher burner wall heat flux for air case and higher rear wall heat flux for oxy case.





**Fig. 12** – Predicted axial temperature profiles for air and oxy-firing with pseudo-air, where oxy-firing has the same primary and secondary momentum as for air-firing.

tion), a similar ignition location to that in air combustion was obtained as shown in Fig. 12. Changes to the burner dimensions and/or to the extent of swirling flow may therefore be required to maintain a similar flame and furnace heat transfer distributions.

## 5. Coal reactivity

In order to predict coal combustion performance using a CFD model in oxyfuel combustion, coal reactivity must be known. Inputs required include high temperature volatile matter release and char reactivity. Laboratory experiments measuring reactivity and volatile yield of coal in air and oxyfuel combustion were completed using +63–90  $\mu\text{m}$  size cuts of the coals used in the pilot-scale tests. Table 2 gives the analysis of the coal samples used.

### 5.1. Drop tube furnace experiments

#### 5.1.1. Volatile matter yield

The coal reactions, including volatile yield and char burnout, of three Australian pulverised coals were measured under simulated air ( $\text{O}_2/\text{N}_2$ ) and oxyfuel ( $\text{O}_2/\text{CO}_2$ ) environments using a drop tube furnace (DTF) maintained at 1673 K (Rathnam et al., 2006, 2007, 2009). The volatile yields of the four coals studied in  $\text{N}_2$  and  $\text{CO}_2$  at 1673 K in the drop tube furnace are shown in Table 5. As seen from Table 5, the high temperature volatile yields ( $V^*$ ) of all coals are higher than their respective volatile yields obtained by the proximate analysis (VM). Therefore, the estimated Q factor which is the ratio of  $V^*$  and VM, is greater than unity. Also, the volatile yields are higher in  $\text{CO}_2$  for all of the four coals studied. The higher volatile yield in  $\text{CO}_2$  is probably due to char- $\text{CO}_2$  gasification

**Table 5** – Volatile yields of coals studied in  $\text{N}_2$  and  $\text{CO}_2$  in the drop tube furnace experiments at 1673 K.

	Coal A	Coal B	Coal C
Proximate analysis			
Volatile matter (a.d.)	25.6	40.5	33.8
$V^*$ ( $\text{N}_2$ )	36.7	52.4	53.5
Q factor ( $\text{N}_2$ )	1.43	1.29	1.58
$V^*$ ( $\text{CO}_2$ )	43.3	55.3	66.2
Q factor ( $\text{CO}_2$ )	1.69	1.36	1.96

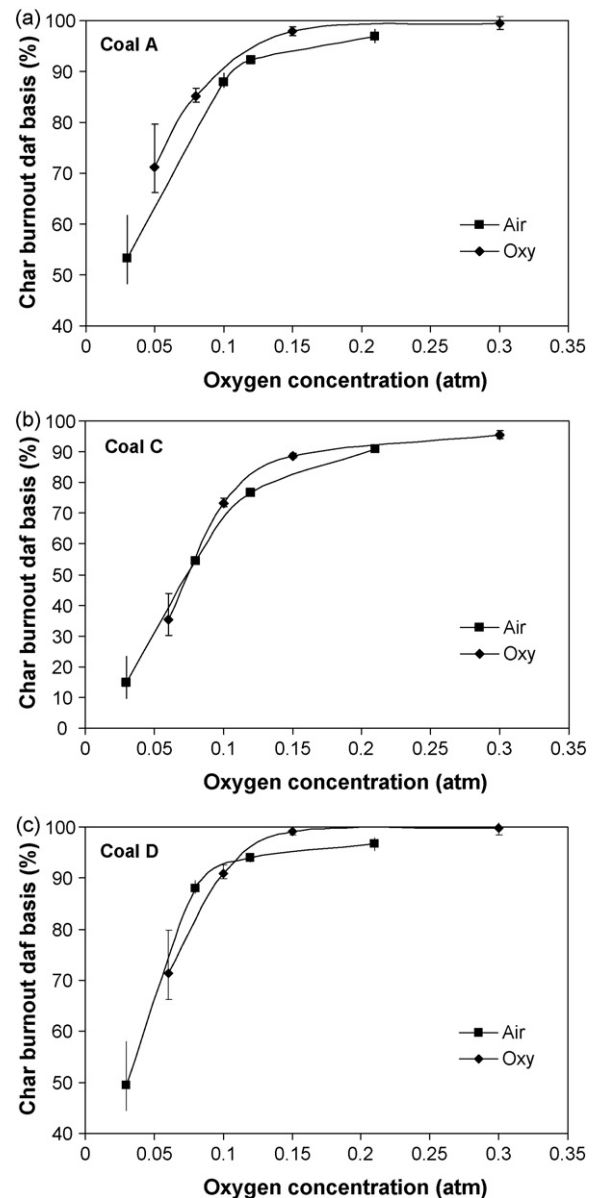


**Fig. 13** – Comparison of char burnout of experimental coals in air and oxy atmospheres in DTF. (a) Coal A; (b) Coal B; (c) Coal C.

in addition to devolatilisation. Following devolatilisation, the char contacts a  $\text{CO}_2$ -rich atmosphere prior to collection where gasification reactions can occur. The true value for devolatilisation may be that measured in  $\text{N}_2$ .

#### 5.1.2. Char reactivity

In order to estimate the char burnout, the volatile yield obtained in  $\text{N}_2$  at 1673 K was subtracted from the measured total coal burnout. Fig. 13(a)–(c) compares the char burnout so estimated, in air and oxyfuel environments, of Coal A to Coal D respectively as a function of  $\text{O}_2$  concentration. Results show that the increase in  $\text{O}_2$  concentration leads to increased char burnout for all the four coals studied. The results also indicate that the char burnout is higher in the oxyfuel atmosphere for almost the whole range of oxygen concentration studied.

This enhancement is attributed to the char gasification reaction with the  $\text{CO}_2$  present. Kinetic parameters for char combustion have been estimated from the burnout data. The reaction orders obtained in this study are in the range of 0.2–0.5. A comparison of reaction rates estimated from

the kinetic parameters obtained from the present study also revealed a higher reaction rate in the oxyfuel atmosphere. The reaction rates decrease with increase in the ash content in char. The present study deals with experimental data obtained at a furnace gas temperature of 1400 °C (Rathnam et al., 2006).

The results are somewhat surprising because most other researchers have found that the reactivity is lower in oxyfuel. Shaddix and Molina (2007) attribute diffusion effects for the reduction in overall combustion rates proposing Regime-III combustion conditions. However, Saastamoinen et al. (1996) have shown that at high temperatures during pressurized pulverised coal combustion, the rate of gasification with CO<sub>2</sub> may become comparable to the rate of diffusion of oxygen through the boundary layer, since there is enough CO<sub>2</sub> available on the surface and inside the particle. The data from the present study also appears to agree with Saastamoinen et al.'s hypothesis. The current data appears to be occurring in Regime-II.

Chars collected from the drop tube furnace pyrolysis experiments in N<sub>2</sub> and CO<sub>2</sub> were examined using scanning electron microscope (SEM) analysis. Particle size analysis determined the swelling of char particles. Both N<sub>2</sub> and CO<sub>2</sub> chars of Coal A appear smaller than the raw coal but have very similar particle size distributions. The N<sub>2</sub> char of Coal B had a mean particle size very similar to that of the raw coal. Both Coal C and Coal D showed significant swelling and the CO<sub>2</sub> char particles were slightly larger than the N<sub>2</sub> char particles. BET CO<sub>2</sub> surface area measurements indicated the surface area of char formed in CO<sub>2</sub> was larger than the surface area of the char produced in N<sub>2</sub>. This is possibly due to the greater exposure of internal surface area created by the char-CO<sub>2</sub> gasification reaction. Coal C and Coal D had a greater surface area increase in comparison to Coal A and Coal B.

## 5.2. TGA study

The thermogravimetric analyser (TGA) run under non-isothermal conditions involving heating at 25 °C/min at temperatures up to 1473 K also has been used to provide coal reactivity under low heating rate conditions (Rathnam et al., 2007, 2009).

### 5.2.1. Volatile matter yield

The pyrolysis reactivity of Coal A was measured in the TGA in both N<sub>2</sub> and CO<sub>2</sub> atmospheres. Fig. 14 shows that the pyrolysis reactivity is very similar in N<sub>2</sub> and CO<sub>2</sub>. The onset of pyroly-

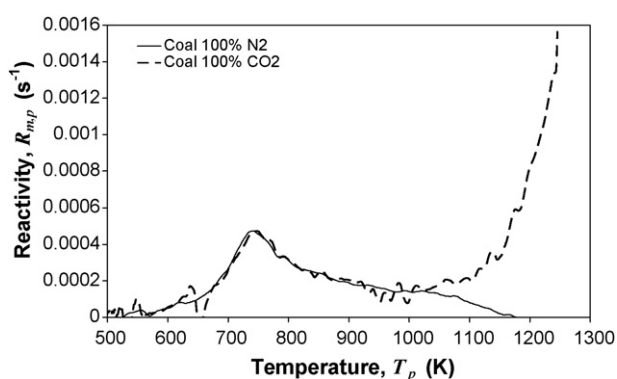


**Fig. 14 – Pyrolysis reactivity of Coal A in N<sub>2</sub> and CO<sub>2</sub>, indicating an increased reactivity in CO<sub>2</sub> at high temperatures.**

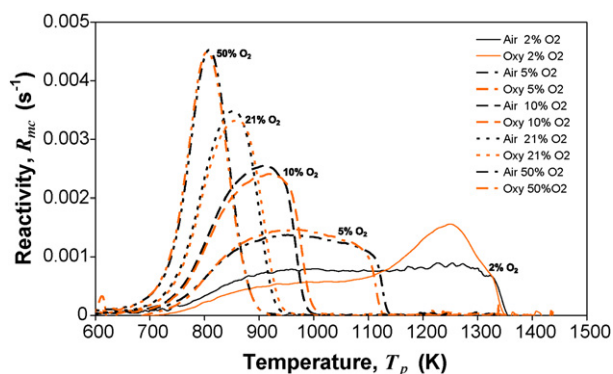


**Fig. 15 – Reactivity comparison of Coal A char, prepared in N<sub>2</sub>, in air and oxy atmospheres in TGA.**

sis occurs at about 573 K. The peak pyrolysis rate occurs at about 750 K in both atmospheres. It could be clearly seen that at around 1030 K the rate of mass loss of the sample in CO<sub>2</sub> starts to increase significantly. This may be due to the commencement of the char-CO<sub>2</sub> gasification reaction. Várhegyi et al. (1996) also observed that the char-CO<sub>2</sub> reaction started at around 1073 K. It appears that the char-CO<sub>2</sub> gasification reaction will play an important role at temperatures >1073 K.

### 5.2.2. Char reactions

The TGA measured reactivity of Coal A char (formed in N<sub>2</sub> at 1673 K in DTF) at various O<sub>2</sub> concentrations in N<sub>2</sub> and CO<sub>2</sub> is shown in Fig. 15. The reactivity of char increases with increasing O<sub>2</sub> concentration in both air and oxyfuel combustion. The char oxidation reaction begins at around 673 K and increases rapidly with the increase in temperature. After reaching a peak value, the reactivity starts to decrease due to the combustion of the less reactive portion of the char. As the O<sub>2</sub> level in the gas increases the peak and burnout temperatures decrease. The char reactivity is slightly less in oxyfuel combustion at 10 and 21% O<sub>2</sub> levels, compared to air combustion. As seen from Fig. 15, the char gasification reaction is not seen in the 5, 10, 21, and 50% O<sub>2</sub> combustion experiments. However, in the 2% O<sub>2</sub> in CO<sub>2</sub> experiment, the reactivity shows a sharp rise when the temperature reaches approximately 1073 K. This char gasification phenomenon is not seen in the higher O<sub>2</sub> experiments, as the burnout of the char is completed at temperatures less than 1073 K (950 K for 21% O<sub>2</sub> and 1000 K for 10% O<sub>2</sub>). This indicates there is competition between O<sub>2</sub> and CO<sub>2</sub> to the gas-char reactions. In oxyfuel combustion in steam generation boilers, the contribution of CO<sub>2</sub> gasification to the carbon loss still has to be clearly identified. It is possible that char-CO<sub>2</sub> gasification could contribute to carbon loss even at higher O<sub>2</sub> levels if the temperature of combustion is above 1073 K.

Várhegyi et al. (1996) found that there was no influence of CO<sub>2</sub> on the reactivity when the O<sub>2</sub> content in the O<sub>2</sub>/CO<sub>2</sub> mixture was varied between 5 and 100%. However, Várhegyi's 5% O<sub>2</sub> experiment (Várhegyi et al., 1996) would also have been completed before reaching the gasification commencement temperature of 1073 K and hence the presence of CO<sub>2</sub> did not influence the reactivity in any of the cases studied. However, the 2% O<sub>2</sub> in CO<sub>2</sub> combustion experiments in the present study does show significant differences in the reactivity upon reaching the gasification temperature. This will have important implications on the burnout of char in a real oxyfuel furnace during the later stages of burnout when the O<sub>2</sub> levels are very low (Stanmore and Visona, 1998).

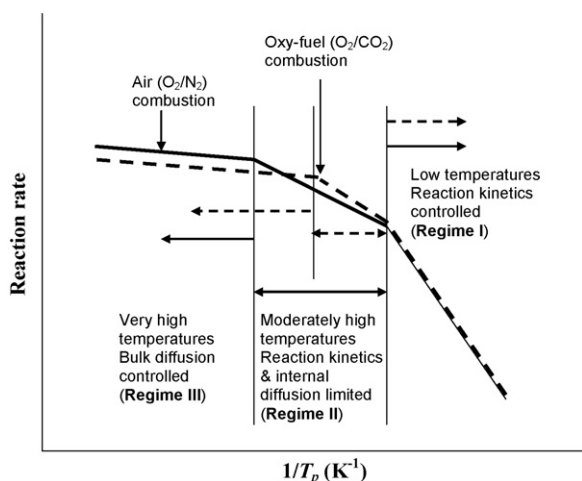


**Fig. 16 – Speculation on the Regimes of combustion in air and oxyfuel atmospheres for the same coal. Solid lines represent air case and dashed lines represent oxy case. The plot for the air case is from typical data. The plot for the oxy case is suggested based on information available in the literature.**

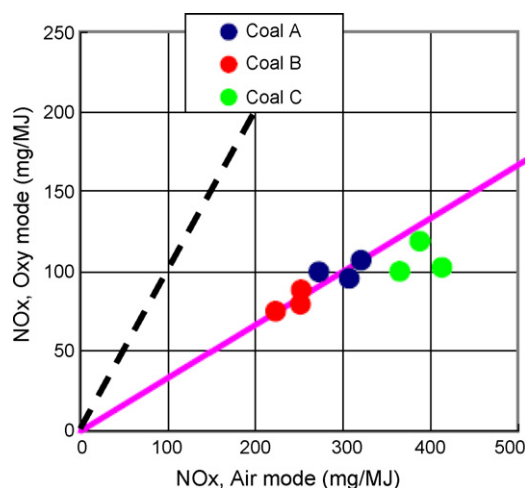
### 5.3. Reactivity at different temperatures

Fig. 16 schematically gives an Arrhenius plot for char combustion in air atmosphere along with its oxyfuel counterpart based on the observations in the literature. Here, for simplicity, the transitions between the Regimes are indicated at defined temperatures, whereas the transitions will occur over a temperature range. In addition the transitions and rates in Regimes II and III will depend on particle size, since this determines the boundary layer thickness and pore length for diffusion. As the particle size is less important than temperature in determining the Regimes for typical pf sizes, Fig. 16 is based only on temperature.

It can be seen from Fig. 16 that in Regime I, the combustion rate is similar in air and oxyfuel combustion. However, as temperatures become moderately high, Regime II conditions are reached. At these temperatures, there may be an additional char- $\text{CO}_2$  gasification reaction which increases the reactivity during oxyfuel combustion conditions. At very high temperatures (Regime III), the combustion rate is limited by the diffusion of  $\text{O}_2$  in the bulk gas. Since the diffusivity of  $\text{O}_2$  is lower in  $\text{CO}_2$  than in  $\text{N}_2$ , lower combustion rates are observed during oxyfuel combustion (Shaddix and Molina, 2007). Fig. 16 is a simplification, other factors such as ash fusion and thermal annealing are also known to limit gasification rates at high temperatures (Liu et al., 2006), and mineral matter in char may also enhance char reactivity with  $\text{CO}_2$  (Harris and Smith, 1990). Moreover, the char formed under oxyfuel conditions may have different properties (swelling index, internal surface area, porosity) that may affect the char reactivity significantly.

The current results add to the previous literature data comparing pf reactivity in air ( $\text{O}_2/\text{N}_2$ ) and oxyfuel ( $\text{O}_2/\text{CO}_2$ ) conditions, but are specific for the four coals tested at the temperatures considered, being 1673 K for coal devolatilised and combusted in a DTF and coal and char from the DTF experiments combusted in a TGA at temperatures less than 1473 K.

From the results, the DTF conditions resulted in char combustion in Regime II, the TGA experiments were in Regime I. The results indicate:



**Fig. 17 – Comparisons of  $\text{NO}_x$  for oxy mode to air mode.**

- The greater mass loss measured during devolatilisation in the DTF experiments in  $\text{CO}_2$  is attributed to the char- $\text{CO}_2$  gasification reaction.
- Char burnout in the DTF were slightly higher in the oxyfuel conditions at the same  $\text{O}_2$  levels.
- Some variations in char swelling and surface area were observed for some chars formed in  $\text{N}_2$  and  $\text{CO}_2$ .

The results are consistent with the Arrhenius plot presented comparing differences in char reactivity in the two conditions.

## 6. Environmental performance

### 6.1. $\text{NO}_x$

Results from the pilot-scale experiments show a 45% increase in concentration (parts per million) of  $\text{NO}_x$  in the flue gas compared to the air-firing  $\text{NO}_x$  concentrations, resulting from the recycling of  $\text{NO}_x$  in the flue gas back to the combustion chamber and a reduction in the total gas flow. However, the mass of  $\text{NO}_x$  released per energy generated is significantly less for oxyfuel combustion conditions as shown in Fig. 17, with approximately one third of the total  $\text{NO}_x$  produced by air combustion.  $\text{NO}_x$  reduction is consistent with the  $\text{NO}_x$  in the recycled gas being reburnt as it contacts the flame generated hydrocarbons and the reducing atmosphere near the flame. This  $\text{NO}_x$  reduction depends on the flame conditions and therefore is expected to be quite variable between experiments.

### 6.2. $\text{SO}_x$

Similarly the  $\text{SO}_2$  in the flue gas (in ppm) of the pilot-scale experiments was directly proportional to the fuel sulphur content in both oxyfuel and air combustion, but it was three times greater in oxyfuel combustion compared to air combustion as shown in Fig. 18. And the concentration did not change significantly with increasing recycle ratio. The total mass (mg/MJ) of sulphur emitted during oxyfuel combustion was two-thirds of the total sulphur in the flue gas of air combustion, and a very small additional decrease in mass of sulphur was observed when the recycle of flue gas through the furnace was increased. The  $\text{SO}_3$  concentration is approximately two and a half (2.5) to three (3.0) times higher in

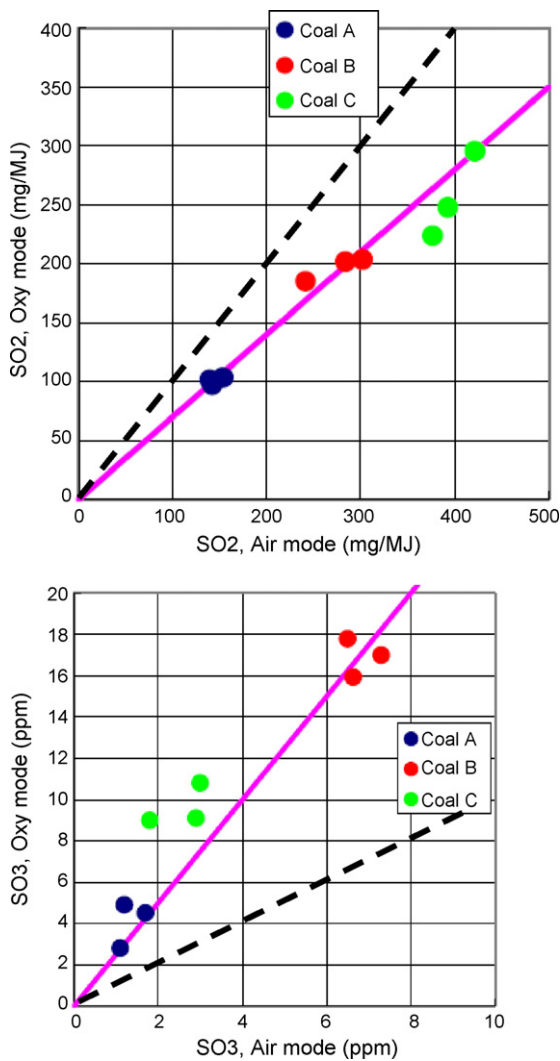


Fig. 18 – Comparisons of  $\text{SO}_x$  for oxy mode and air mode.

oxyfuel combustion than in air combustion as shown in Fig. 18.

In general the fly ash produced during oxyfuel combustion contained slightly more sulphur and the furnace deposits contained significantly more sulphur compared to air combustion samples. This is consistent with the higher  $\text{SO}_2$  and  $\text{SO}_3$  concentration levels measured.

The mass balance of the coal ash could not be closed as a significant proportion of the ash was not accounted for in the experiment. It appears that ash was depositing throughout the furnace, or lost in ducts, which contained a significant proportion of the coal sulphur. Deposition of sulphurous species due to elevated gas phase  $\text{SO}_3$  concentrations in oxyfuel combus-

tion is expected to increase the amount of furnace corrosion experienced. The acid dew point was shown to be increased under oxyfuel combustion conditions further increasing the potential corrosion during operation, which may result in the need for desulphurisation of the flue gas or limit oxyfuel combustion to low sulphur coals.

### 6.3. Ash

Due to the reduced gas volume in oxyfuel combustion, the dust concentration measured is 1.5 times greater than during air combustion, with no significant difference in the dust particle size distribution. The particle diameter of fly ash was approximately  $5\ \mu\text{m}$  for Coal A and Coal C, and approximately  $8\text{--}10\ \mu\text{m}$  for Coal B when produced during both air and oxyfuel combustion. Fig. 19 shows the chemical composition of ash appears to be only affected if changes in the flame temperature alter the character of particles which affects ash deposition. The chemistry of collected deposit samples indicated oxyfuel deposits contained more sulphur than air deposits, though fly ash samples from both combustion modes had similar sulphur contents.

The bottom ash from Coal A and Coal C was finer when produced in oxyfuel conditions due to the reduced gas flow (lower gas velocity) which would not be able to support larger ash particles. This indicates the amount of bottom ash produced in oxyfuel combustion will increase compared to the quantity produced in air combustion.

### 6.4. Trace elements

Different trends were produced for trace element emissions during oxyfuel and air combustion. The proportion of mercury that reported to the ash for Coal B and Coal C increased during Oxyfuel combustion. However, none of this mercury appeared to be leachable. The form of the mercury present was not determined.

The coals contained higher proportions of some trace elements compared to the average value for export Australian coals:

Coal A contained relatively high concentrations of lead, chromium, manganese, nickel and thorium. All of these species were retained in the fly ash.

Coal B contained relatively high concentrations of lead, vanadium, molybdenum and zinc. A proportion of zinc and molybdenum was found to be leachable from the fly ash, with more zinc and less molybdenum extracted from the oxyfuel combustion ash compared to the air combustion ash.

Coal C contains high proportions of boron but low concentrations of mercury, chlorine and selenium, vanadium, zinc,

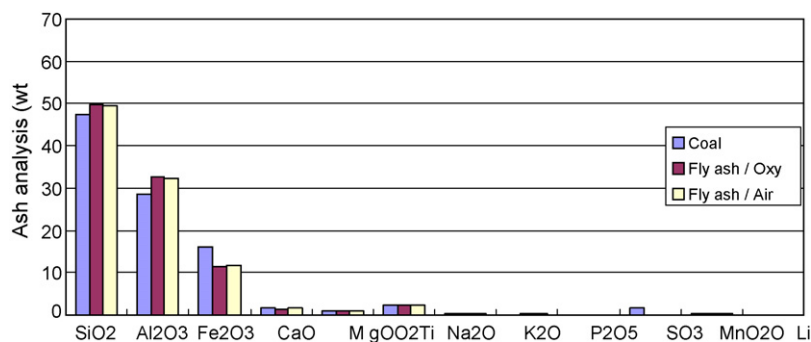


Fig. 19 – A comparison of ash chemistry for Coal A, fly ash from air combustion and oxyfuel combustion respectively.

cadmium, chromium, copper and lead. Boron was found in both the fly ash and the flue gas. Both air combustion and oxy-fuel combustion bag filter ash contained similar amounts of boron but twice the amount of boron was leached from oxyfuel combustion ash.

The Coal A oxyfuel combustion fly ash also captured higher amounts of chlorine and slightly more vanadium, while it contained less fluoride and zinc. A higher proportion of vanadium and a smaller proportion of this zinc were leachable from the oxyfuel combustion ash. Coal B oxyfuel combustion fly ash captured less chlorine and significantly more mercury during oxyfuel combustion. And Coal C oxyfuel combustion fly ash captured higher amounts of chlorine, mercury and zinc. More selenium, molybdenum and arsenic were leached from the air combustion ash and more cadmium, zinc and copper were leached from the oxyfuel combustion ash.

No systematic study on trace element deportment has been reported for comparison.

## 7. Conclusions

Three Australian coals have been studied in furnaces at laboratory scale and pilot-scale facilities experimentally and using mathematical modelling to compare and interpolate the difference in air combustion and oxyfuel combustion. Heat transfer, coal reactivity and emissions in oxyfuel combustion differ from air combustion because of differences in combustion conditions resulting from reduced volumetric flue gas, enhanced oxygen level and recycled flue gas.

The research has made several contributions to knowledge, including:

- New measurements in a pilot-scale oxyfuel furnace comparing temperatures, burnout, and gas compositions have been obtained simulating air-firing retrofitted to oxyfuel, when furnace heat transfer is matched.
- The use of AFT as a design criterion for furnace design for an oxy retrofit has been evaluated, and modified with a criterion of matching heat transfer considered more appropriate.
- The emissivity of the gases in oxy-fired furnaces has been predicted by a new 4-grey gas model, which is required as a furnace model input for CFD predictions.
- The first measurements of coal reactivity comparisons, including high-temperature volatile yields and coal burnout, at several O<sub>2</sub> levels in air and oxyfuel combustion conditions at pilot-scale and laboratory scale have been obtained, showing a higher reactivity in oxyfuel at the same O<sub>2</sub> concentrations.
- Observed delays in flame ignition in oxy-firing has been shown by mathematical modelling to be due to both gas property differences and aerodynamic effects, due to the differing momentum flux ratio of primary to momentum levels associated with a retrofit.

## Acknowledgements

The authors wish to acknowledge the financial support provided by the Cooperative Research Centre for Coal in Sustainable Development, which is funded in part by the Cooperative Research Centres Program of the Commonwealth Government of Australia. The pilot-scale experiments were supported financially by ACARP, xstrata coal, and CCSD.

## References

- Abele, A.R., Kindt, G.S., Clark, W.D., Payne, R. and Chen, S.L., (1987). *An Experimental Program to Test the Feasibility of Obtaining Normal Performance from Combustion using Oxygen and Recycled Gas Instead of Air*. (Argonne National Laboratory). ANL/CNSV-TM-204, DE89-002383, p. 177
- Abraham, B.M., Asbury, J.G., Lynch, E.P. and Teotia, A.P.S., 1982, Oil & Gas Journal, 80(11): 68–70.
- Allam, R.J., White, V., Panesar, R.S. and Dillon, D., 2005, Optimising the design of an oxyfuel-fired advanced supercritical PF boiler, in Proceedings of the 30th International Technical Conference on Coal Utilization & Fuel Systems. Coal Technology: Yesterday–Today–Tomorrow, April 17–21, Sakkestad, B.A. (ed). (Coal Technology Association, Clearwater, FL, USA)
- Berry, G. and Wolsky, A., 1986, Modeling heat transfer in an experimental coal-fired furnace when CO<sub>2</sub>/O<sub>2</sub> mixtures replace air, In *Winter Annual Meeting* (pp. 86-WA/HT51). (ASME)
- Buhre, B.J.P., Elliott, L.K., Sheng, C.D., Gupta, R.P. and Wall, T.F., 2005, Progress in Energy and Combustion Science, 31: 283–307.
- Croiset, E., Douglas, P.L. and Tan, Y., 2005, Coal oxyfuel combustion: a review, In *Proceedings of the 30th International Technical Conference on Coal Utilization & Fuel Systems—Clearwater Coal Conference* Clearwater, FL, USA,
- Edwards, D.K. and Matavosian, R., 1984, Journal of Heat Transfer, 106: 684.
- Gupta, R.P. and Wall, T.F., 1985, Combustion and Flame, 61: 145–151.
- Gupta, R., Khare, S., Wall, T., Spero, C., Eriksson, K., Lundström, D. and Eriksson, J., 2006, Adaptation of gas emissivity models for CFD based radiative transfer in large air-fired and oxy-fired furnaces, in Proceedings of the 31st International Technical Conference on Coal Utilization & Fuel Systems, May 21–26, Sakkestad, B.A. (ed). (Coal Technology Association, Sheraton Sand Key, Clearwater, FL, USA)
- Harris, D.J. and Smith, I.W., 1990, (The Combustion Institute), pp. 1185–1190.
- Hottel, H.C. and Sarofim, A.F., (1967). *Radiative Transfer*. (McGraw-Hill, New York), p. 520
- IPCC Intergovernmental Panel on Climate Change. <http://www.ipcc.ch> (September 27, 2007).
- Katzer, J., 2007. The future of coal: an interdisciplinary MIT study. MIT report; p. 192.
- Khare, S., (2008). *Heat Transfer in Oxyfuel Combustion*. (Doctor, the University of Newcastle, Newcastle).
- Khare, S., Wall, T., Gupta, R., Elliott, L. and Buhre, B., 2005, Retrofitting of air-fired PF plant to oxy-fuel and associated oxygen levels through the burners and oxygen production requirements, in Proceedings of the 30th International Technical Conference on Coal Utilization & Fuel Systems. Coal Technology: Yesterday–Today–Tomorrow, April 17–21, Sakkestad, B.A. (ed). (Coal Technology Association, Clearwater, FL, USA), p paper 69
- Khare, S.P., Wall, T.F., Farida, A.Z., Liu, Y., Moghtaderi, B. and Gupta, R.P., 2008, Fuel, 87: 1042–1049.
- Kiga, T., 2001, in Miura, T. (ed) (Nova Science Publishers Inc, Huntington, NY), pp. 185–241.
- Kiga, T., Takano, S., Kimura, N., Omata, K., Okawa, M., Mori, T. and Kato, M., 1997, Energy Conversion and Management: Proceedings of the Third International Conference on Carbon Dioxide Removal, pp. S129–S134, 38 (Supplement 1)
- Kimura, N., Omata, K., Kiga, T., Takano, S. and Shikisima, S., 1995, Energy Conversion and Management: Proceedings of the Second International Conference on Carbon Dioxide Removal, pp. 805–808, 36 (6–9)
- Leckner, B., 1972, Combustion and Flame, 19: 33–48.
- Liu, H., Luo, C., Kato, S., Uemiya, S., Kaneko, M. and Kojima, T., 2006, Fuel Processing Technology, 87: 775–781.
- Ludwig, C.B., Malkmus, W., Reardon, J.E. and Thompson, J.A., (1973). *Handbook of Infrared Radiation from Combustion Gases*. (NASA). SP-3080
- Lundström, D., Eriksson, J., Anheden, M., Gupta, R., Wall, T. and Spero, C., 2006, The use of CFD modeling to compare air and

- oxy-firing of a retrofitted pulverized fuel boiler, in Proceedings of the 31st International Technical Conference on Coal Utilization & Fuel Systems, May 21–26, Sakkestad, B.A. (ed) Clearwater, FL, USA. (Coal Technology Association)
- Nakayama, S., Noguchi, Y., Kiga, T., Miyamae, S., Maeda, U., Kawai, M., Tanaka, T., Koyata, K. and Makino, H., 1992, *Energy Conversion and Management*, 33(5–8): 379–386.
- Nozaki, T., Takano, S., Kiga, T., Omata, K. and Kimura, K., 1997, *Energy*, 22(2/3): 199–205.
- Payne, R., Chen, S.L., Wolsky, A.M. and Richter, W.F., 1989, *Combustion Science and Technology*, 67: 1–16.
- Rathnam, R.K., Elliott, L., Moghtaderi, B., Gupta, R. and Wall, T., 2006, Differences in coal reactivity in air and oxy-fuel conditions and implications for coal burnout, in Proceedings of the 31st International Technical Conference on Coal Utilization & Fuel Systems, May 21–26, Sakkestad, B.A. (ed) Clearwater, FL, USA. (Coal Technology Association)
- Rathnam, R.K., Moghtaderi, B. and Wall, T., 2007, Differences in pulverised coal pyrolysis and char reactivity in air ( $O_2/N_2$ ) and oxy-fuel ( $O_2/CO_2$ ) conditions, in Proceedings of the 32nd International Technical Conference on Coal Utilization & Fuel Systems, June 10–15, Sakkestad, B.A. (ed) Clearwater, FL, USA
- Rathnam, R.K., Elliott, L., Wall, T., Liu, Y., Moghtaderi, B., 2009. *Fuel Processing Technology*, in press.
- Khare, S., Wall, T., Abdulgani, Z., Liu, Y., Moghtaderi, B. and Gupta, R., 2007, Comparison of the ignition of oxy-fuel and air-fired PF flames, In *Proceedings of the 24th Annual International Pittsburgh Coal Conference*, September 10–14. (Sandton Convention Centre, Johannesburg, South Africa)
- Khare, S.P., Farida, A.Z., Wall, T.F., Liu, Y. and Moghtaderi, B., 2007, Factors influencing the ignition of flames from air fired swirl PF burners retrofitted to oxy-fuel, in Proceedings of the 32nd International Technical Conference on Coal Utilization & Fuel Systems, June 10–15, Sakkestad, B.A. (ed) Clearwater, FL, USA
- Saastamoinen, J.J., Aho, M.J. and Hamalainen, J.P., 1996, *Energy & Fuels*, 10: 121–133.
- Santos, S., Haines, M. and Davison, J., 2006, Challenges in the development of oxy-combustion technology for coal fired power plant, in Proceedings of the 31st International Technical Conference on Coal Utilization & Fuel Systems, Sakkestad, B.A. (ed). (Coal Technology Association, Sheraton Sand Key, Clearwater, FL, USA), p. 1
- Shaddix, C.R. and Molina, A., 2007, Influence of  $CO_2$  on coal char combustion kinetics in oxy-fuel applications, In *Proceedings of the 5th US Combustion Meeting Organized by the Western States Section of the Combustion Institute*. (The University of California at San Diego, 2007, The University of California at San Diego)
- Smith, T.F., Shen, Z.F. and Friedman, J.N., 1982, *Journal of Heat Transfer*, 104: 602–608.
- Spero, C., 2007, Status of calide (30 MWe) oxyfuel project, In *2nd Workshop of the Oxy-fuel Combustion Network*, January 25–26. (Hilton Garden Inn, Windsor, Connecticut)
- Stanmore, B.R. and Visona, S.P., 1998, *Combustion and Flame*, 113: 274–276.
- Wall, T., 2007, Performance of PF burners retrofitted to oxy-firing, In *2nd Workshop of the Oxy-fuel Combustion Network*, January 25–26. (Hilton Garden Inn, Windsor, Connecticut)
- Wall, T.F., 2007, Combustion processes for carbon capture, In *Proceedings of the Combustion Institute*, pp. 31–47
- Várhegyi, G., Szabó, P., Jakab, E. and Till, F., 1996, *Energy & Fuels*, 10: 1208–1214.
- Wall, T., 2005, Fundamentals of oxy-fuel combustion, In *Inaugural Workshop of the Oxy-fuel Combustion Network*, November 29–30 Cottbus, Germany,
- Wang, C.S., Berry, G.F., Chang, K.C. and Wolsky, A.M., 1988, *Combustion and Flame*, 72: 301–310.
- Weller, A.E., Rising, B.W., Boiarski, A.A., Nordstrom, R.J., Barrerr, R.E. and Luce, R.G., (1985). *Experimental Evaluation of Firing Pulverized Coal in a  $CO_2/O_2$  atmosphere*. (Argonne National Laboratory). ANL/CNSV-TM-168
- White, C.M., Strazisar, B.R., Granite, E.J., Hoffman, J.S. and Pennline, H.W., 2003, *Journal of the Air & Waste Management Association*, 53(6): 645–715.
- Yamada, T., Tamura, M., Fujimori, T., Khare, S., Wall, T.F., Isherwood, B. and Spero, C., 2006, Comparison of combustion characteristics of between oxy-fuel and air combustion, in Proceedings of the 31st International Technical Conference on Coal Utilization & Fuel Systems, May 21–26, Sakkestad, B.A. (ed). (Coal Technology Association, Sheraton Sand Key, Clearwater, FL, USA), p. 17